Journal of Applied Mechanics and Technical Physics, Vol. 40, No. 5, 1999

SUSPENDED DISCONTINUITIES IN THE FIELD OF TWO-DIMENSIONAL INTERNAL WAVES

V. V. Mitkin and Yu. D. Chashechkin

UDC 532.5:681.7

Using various shadow methods of visualization for a stratified flow near a horizontal cylinder towed with constant velocity, a new structural element of the flow, namely, the isolated high-gradient interlayers in the field of attached internal waves, is identified. In their basic characteristic features, these layers may be viewed as those belonging to the class of inner boundary layers which are the prevalent mechanism for formation of the fine structure of a continuously stratified medium. The data on optical visualization are confirmed by direct measurements of the electrical conductivity.

Many experimental and theoretical studies (see, e.g., [1–3]) are devoted to the structure of a stratified flow around a horizontal cylinder which is of both theoretical and applied interest. The essential elements of a two-dimensional flow, such as the propagating upstream disturbances, the wake past a body, and the suspended vortices, play an important role in the dynamics of natural systems (the ocean and atmosphere) [4].

Originally, main attention was paid to the study of attached internal waves past a cylinder in a fluid with constant [5] or varying (discontinuous) density gradient [6]; later, attention was focused on obtaining diagrams of rotational flow regimes [7, 8]. The jumps in the density gradient that appear at the outer boundary of the wake [9] strengthen the effect of weak stratification and affect its spatial structure and stability [10].

A fine-structure boundary flow with various scales of spatial variations of velocity and density is developed even near a fixed obstacle because of interruption of the molecular flux of the stratifying component [11]. Separation of these flows produces high-gradient shells of the density wake which was observed in experiments [9, 10]. However, thin high-gradient interlayers (the "traumas of stratification) can appear not only near a relief due to separation of the boundary flow but also directly inside the fluid, for example, in the regions of intersection of the intense beams of internal waves [12, 13]. The discontinuities in the stratification are also observed in the wake behind the isolated vortices which appear after breaking of the attached internal waves [3, 4, 8]. In this connection, it is of interest to study the fine flow structure near the boundaries of the existence region of suspended vortices in the space of basic dimensionless parameters of the problem where the dimensions of the vortices are minimal.

Analysis of the linearized equations of motion that take account of viscosity and diffusion shows that, together with internal waves, inside a fluid there can exist inner boundary flows whose thickness is determined by the appropriate kinetic coefficients and the buoyancy frequency, and whose form and dimension are determined by the geometry and energetics of the problem [14]. This type of flow can appear both owing to separation of a split boundary flow [9, 10] and directly within the thickness of the continuously stratified fluid. In the latter case, these flows must be in the form of isolated planar or linear discontinuities of the density gradient (as in the regions of intersection of monochromatic waves [12, 13]). The purpose of this paper is an experimental verification of the possibility of forming high-gradient interlayers in the attached internal waves and a study of the range of parameters where they exist.

Institute of Problems of Mechanics, Russian Academy of Sciences, Moscow 117526. Translated from Prikladnaya Mekhanika i Tekhnicheskaya Fizika, Vol. 40, No. 5, pp. 40–50, September–October, 1999. Original article submitted February 16, 1998.

Basic Parameters. The dimensional parameters of the problem are the density ρ_0, its gradient $d\rho_0/dz$, the kinematic viscosity ν, the diffusion coefficient of salt $k_s = 1.4 \cdot 10^{-5}$ cm^2/sec (for aqueous solution of sodium chloride), the velocity U, the body diameter D, the acceleration of gravity g, and the buoyancy length scale $\Lambda = |d(\ln \rho_0)/dz|^{-1}$ (the z axis is vertical). The basic characteristic scales of the problem (apart from the external parameters such as the dimensions of the body and the buoyancy length scale) are the dimensions of the main structural elements of the flow: the wavelength of the attached internal wave $\lambda = UT_b = 2\pi U/N$ ($T_b = 2\pi/N = 2\pi\sqrt{\Lambda/g}$ is the buoyancy period, where N is the buoyancy frequency), the thickness of the velocity boundary layer $\delta_u = \nu/U$, and the thickness of the density boundary layer $\delta_\rho = k_s/U$. The thickness of the inner boundary flow is $\delta_\nu = \sqrt{\nu/N}$ and the thickness of the density inhomogeneity related to this flow is $\delta_s = \sqrt{k_s/N}$ [14]. The ratios of the basic scales yield the characteristic dimensionless parameters: the Reynolds number $\mathrm{Re} = D/\delta_u = UD/\nu$, the Peclet number $\mathrm{Pe} = D/\delta_\rho = UD/k_s$ (or the Schmidt number $\mathrm{Sc} = \mathrm{Pe}/\mathrm{Re}$), the internal Froude number $\mathrm{Fr} = \lambda/(2\pi D) = U/(ND)$, and the ratio between the length scales $C = \Lambda/D$. Since the stratification is weak and the kinetic coefficients are quite small, the basic characteristic parameters differ considerably ($\Lambda \gg D \gg \delta_u \gg \delta_\rho$ and $\lambda \gg \delta_\nu \gg \delta_s$). The smallest basic length scale (δ_ρ or δ_s) determines the spatial resolution that is necessary for observation of these elements of the flow. Since the location of the fine-structure elements of the flow is not known in advance, the registration method must involve a sufficiently large observation region. In practice, these requirements are satisfied only by high-quality shadowgraphs.

The experiments were carried out in the range of parameters where the vertical dimensions of the wake are the smallest dimensions. In particular, this is satisfied for the regime of "isolated vortex patches on the wake axis" ($0.2 < \mathrm{Fr} < 1$ and $50 < \mathrm{Re} < 500$) [7, 8]. In this case, the attached internal waves do not break.

The Technique. The experiments were performed in a 220 × 40 × 60 cm tank with transparent walls which was filled with a linearly stratified aqueous solution of sodium chloride by the continuous displacement method. Before each experiment, the buoyancy period was measured by registering the oscillations of the density mark with an electrical-conductivity probe (with an error not greater than 5%). In the present experiments, $T_b = 5.0$–20.5 sec.

The flow pattern past a horizontal cylinder of diameter $D = 1.5$, 2.5, and 7.6 cm was studied. The cylinder was towed with a constant velocity in the middle region of the pool. The cylinder was attached by thin blades to a carriage which was moved along the guide fence with the velocity $U = 0.05$–1.00 cm/sec. In the diagram of [7, 8], the conditions of these experiments ($C = 450$–1500, $\mathrm{Fr} = 0.01$–0.50, and $\mathrm{Re} = 50$–100) correspond to the "isolated vortex patches on the wake axis" and "the wake with closed high-gradient core" regimes. Before each experiment, the cylinder was placed near the end wall of the tank.

Visualization was performed with an IAB-458 shadowgraph by Maksudov's method in several ways: a vertical slit producing a thin light sheet, a slit producing a thread in focus, and a horizontal slit producing a lattice in focus. The two first methods produce black-and-white images whose brightness is proportional to variations of the horizontal component of the refraction coefficient (for the light-sheet method) or its absolute value (for the thread method). The lattice that exploits the natural dispersion of light forms a system of color strips whose displacement is proportional to the vertical component of the gradient of the refraction coefficient [15]. The spatial resolution of these methods is almost the same and does not exceed 0.1 mm in the case of photographic registration.

The shadowgraphic images obtained by different methods are not similar. The light-sheet method is the most sensitive method, but the wave images that are beyond the working range of the device overshadow the lower-contrast small-scale elements of the flow. The thread method visualizes only the lines of wave crests and troughs (whose images are different) and makes it possible to register the finer structures on their background. The sensitivity and resolution of the color shadow method can be adjusted by changing the lattice spacing and the type of lattice. Thus, the use of three independent techniques improves the accuracy and reliability of the results.

Most of visualization data are confirmed by contact measurements of the electrical conductivity. The equation of state which relates the density and electrical conductivity of an aqueous solution of sodium chloride

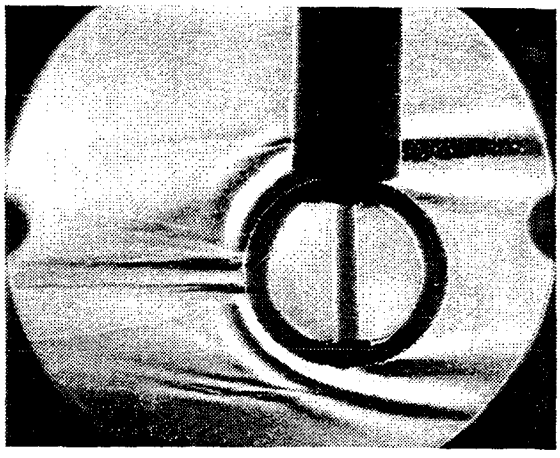

Fig. 1

is usually linearized [16]. The design of the probe and the method of its static and dynamic calibration are described in details in [17].

Main Results. The typical photogram of the flow near a horizontal cylinder moving from left to right in a weakly stratified medium is shown in Fig. 1 (T_b = 20.5 sec, D = 7.6 cm, U = 0.05 cm/sec, Fr = 0.02, Re = 38, and C = 1370). Visualization was carried out by the light-sheet method. Since the Froude number is less than the critical number which, in turn, is a function of the Froude number and the ratio of the length scales, the wake is laminar. The Froude number is also small, so that only the first two attached waves are meaningful in these conditions. Their phase surfaces past the body are the semicircumferences which smoothly become inclined straight lines ahead of the body; these lines are the image of unsteady internal waves.

The wavelength is determined by the velocity of a cylinder and the local buoyancy frequency $\lambda = 2\pi U/N$ and does not depend on the diameter of the body [2, 4, 17]. Apart from the waves, the important elements of the flow pattern are the surfaces of discontinuities of the density gradient, which appear as thin dark and light lines in the shadow photograms. In this regime, inside the laminar wake one observes two sets of discontinuities of the density gradient which come in contact with the body surface near the rear stagnation point. These sets of attached discontinuities are produced by both separation points of the two-dimensional density boundary layer, which are at the distance Δz = 0.7 cm from the plane of motion of the cylinder axis.

The inner horizontal interlayers (dark lines in Fig. 1) outline the vortex core of the wake in which the fluid velocity can exceed the velocity of the body. The outer, inclined shells (light inclined lines) separate the wake and the field of attached internal waves. Both the form and the thickness of the boundary of the wave zone in the region of its contact with the density-wake shell are determined by the density-jump layer geometry (rather than by the wavelength). Therefore, the interaction between the internal waves and the high-gradient shells is strong.

The outer boundaries of the density wake approach the separation point at the angle $\varphi = 26°$ to the horizon. The angular position of the separation points reckoned from the rear stagnation point is $\theta = 10°$. The thickness of the boundary of the wake (dark diffuse horizontal strips in Fig. 1) is δ_c = 1.4 mm and remains almost unchanged when the distance from the body increases. The thickness of the outer discontinuity does not exceed δ_b = 0.7 mm and is near the limits of spatial resolution of the method (taking account of the film grain).

The geometry of the density wake allows us to identify three masses of water with various densities and various spatial density distributions. A fluid that appear in the outer part of the wake flows over an obstacle and passes from an upstream to a downstream perturbation. This fluid is lighter in the upper half-space and heavier in the lower half-space compared to the unperturbed medium. The inner core of the wake contains a fluid with the initial density distribution that comes from remote regions past the body. The region between these two high-gradient shells is filled with a fluid of intermediate density.

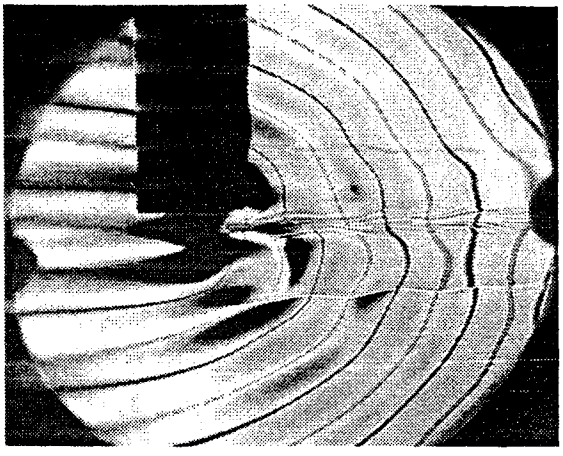

Fig. 2

Thus, even in a laminar flow of a homogeneous fluid ($\mathrm{Re} < \mathrm{Re}_{cr}$, $\mathrm{Re} = 38$, and $\mathrm{Re}_{cr} = 60$ [18]) the wake past the cylinder has a nontrivial structure and the flow is rotational. The high-gradient interlayers are the boundaries of vortices, and this is typical of continuously stratified media [19, 20].

In the photograph (Fig. 1), one can identify two other groups of small-scale inhomogeneities, namely, the high-gradient interlayers (suspended discontinuities of the density gradient) which are in the field of attached internal waves. These features of the flow were not yet mentioned in the literature [2–5].

In the lower part of the shadow photogram obtained by the Foucault method (Fig. 1), the interlayers correspond to the group of two light and dark strips with total thickness $\delta_t = 0.85$ cm and length $l \approx 7.8$ cm; they are inclined at an angle $\beta = 8°$ to the horizon. The other methods of visualization yield the same dimensions of this region. In particular, the thickness of the fine-structure region that is visualized by the thread method is 0.85 cm, and its length is 7.8 cm. In the upper half-space, the same structure does not have good contrast, because it is overshadowed by the perturbations caused by the supporting blades.

The sharp leading edge of the high-gradient structures is located in the neighborhood of the crest of the second attached wave in the upper half-space (one can see troughs in the lower half-space, because the field of attached internal waves is antisymmetric relative to the plane of motion of the body). In Fig. 1, the angular position of the leading edges of the structures reckoned from the rear stagnation point is $\alpha = 87°$. The coordinates of the leading edge of the interlayer relative to the center of the body are $x = 0.6$ cm and $y = 4.6$ cm. The distance from the body surface to the interlayer is $r = 0.9$ cm.

Molecular diffusion smoothens the gradients along the interlayer, and, therefore, the rear edge of the structure is less sharp than the leading edge. The thickness of separate elements of this inhomogeneity is not more than $\delta = 1.5$ mm, and this is considerably less than the length of the attached internal wave $\lambda = 1.1$ cm for this experiment.

Structures of this type are reproduced and observed for quite a wide range of flow parameters. As an example, Fig. 2 shows the pattern of a flow past a cylinder of smaller diameter which moves from right to left in a medium with a high buoyancy frequency in the regime of "isolated vortex patches" [7, 8] ($T_b = 6$ sec, $D = 1.5$ cm, $U = 0.52$ cm/sec, $\mathrm{Fr} = 0.33$, $\mathrm{Re} = 78$, and $C = 600$). In this range of parameters, the generation of waves is quite effective, many waves are observed, and the region occupied by the waves is considerably larger than the field of view of the shadowgraph.

The form of constant phase surfaces, in particular, the crests and troughs of the attached internal waves, is not perfect (semicircumferences past the body in Fig. 2) only in the shear-flow region inside the velocity wake. When the traditional shadowgraph visualization is used, the crests and troughs of the waves are at the boundaries between the light and dark strips (see Fig. 1). When the thread method is used, the images of the wave crests and troughs differ one from another (see Fig. 2). The darker solid lines correspond to wave crests, and the double gray lines are associated with wave troughs. The maximum deviation from

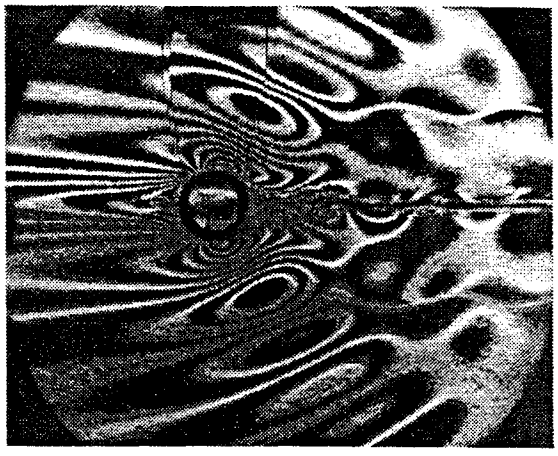

Fig. 3

the circular form is observed in the neighborhood of the regions of density wake expansion bounded by the fine-structure interlayers.

The wave field is spatially inhomogeneous. The first two groups of waves separated by the density wake are antisymmetric, and the subsequent ones penetrate the density wake. Although the similar phase surfaces (crest–crest and trough–trough) are closed with one another, the positions of the crests and the troughs in an unperturbed space remain unchanged and are in agreement with the linear theory [2, 3].

In the present case, inside the wave field there are two systems of discontinuities the images of which in Fig. 2 are long wavy curves (dark in the upper half-space and light in the lower half-space) located at the distance $y = 2.6$ cm from the line of motion of the center of the body. Their thickness $\delta = 0.7$ mm is practically constant over the length, and their form reflects the distribution of wave displacements of the particles. In these interlayers, the phase surfaces of the attached internal waves have discontinuities, which are clearly seen in the form of displacements in the last three waves in the lower half-space in the left part of the frame. In this regime, the leading edge of the suspended isolated discontinuities is far from the body ($x = 1$ cm and $y = 2.6$ cm), but is located on the same phase surface as in the previous case. The angular position of the leading edge of the interlayer reckoned from the rear stagnation point is $\alpha = 70°$. The interlayer length is $l > 13$ cm or $l/\lambda > 4$ in relative units. The ratio of the length of the interlayer to its thickness is $l/\delta > 180$. In this regime, the length of the suspended isolated discontinuities notably exceeds the dimensions of the field of view.

The black-and-white picture of the color shadow image of a flow past a cylinder moving from right to left is shown in Fig. 3 ($T_b = 12.5$ sec, $D = 2.5$ cm, $U = 0.3$ cm/sec, Fr $= 0.24$, Re $= 76$, $C = 1500$, and a uniform lattice with a spacing of 1.5 mm). Apart from the waves propagating upstream and the wake with the bottom vortex and isolated vortex patches, this method makes it possible to observe the high-gradient density boundary layer on the body in the form of close isolines near the upper and lower poles of the body. Analysis of the photograms shows that the color shadow method allows one to obtain additional information not only on the geometry of the structural elements, but also on the relative variations of the density gradient in them.

In particular, the distribution of isolines of the field of internal waves in the color photogram characterizes the magnitude of displacements along the phase surfaces. The distribution of displacements along a particular phase surface is not monotonic. One can clearly see the gullies and troughs whose dimensions and angular positions depend on the effective size of the region of wave generation, the wave number, and the basic parameters of the problem. In the present case, the regions of maximum wave perturbations (the centers of the elliptic light and dark rings) are located on the straight lines passing through the center of the body and inclined at the angles $\psi_1 = 60$ and 65° to the horizon for the first wave and $\psi_2 = 55°$ for the second wave; this agrees with the models proposed in [4, 21].

The form and character of the concentration of isolines allow us to identify the region of the blocked fluid and the contact points of its boundary with the body (this method visualizes bifurcation points on both the front and rear parts of the body). The angular position of the front bifurcation point reckoned from the front stagnation point is 60°, and that of the rear bifurcation point reckoned from the rear stagnation point is 35°.

In the present frame, the isolated interlayers, which are a natural extension of one of the isolines of the wave field, can be seen in the form of light wavy curves of thickness $\delta = 1.5$ mm which continue far along the wake beyond the frame. They are located at the distance $y = 3.5$ cm from the line of motion of the center of the body. In the present series of experiments, the concentration of the isolines that marks the line of gradient growth starts for $C = 1500$, Fr $= 0.17$, and Re $= 56$. When the velocity of the body increases, the length of the suspended discontinuities and the density jump at them grow simultaneously, and their angle of inclination to the horizon decreases. The interlayer has the highest contrast for $C = 1500$, Fr $= 0.24$, and Re $= 76$. With further increase in the velocity, their contrast weakens and the interlayers are not distinguished from the wave background for $C = 1500$, Fr > 0.3, and Re > 95. At the same time, there are no qualitative changes in the other elements of the structure.

This method of observation does not show any specific features or compact vortices on the leading edges of these interlayers. In all the experiments, the suspended discontinuities and the obstacle are separated by a fluid layer with continuous variation in all the parameters.

Analysis of the displacements of the density marker shows that the suspended discontinuities of the density gradient are located in the regions of maximum velocity shear outside the density wake. In the present experiments, the scale of velocity variations $l_u = (d\ln(u)/dz)^{-1} = 4.7$ cm is considerably larger than the interlayer thickness, which does not exceed 1.5 mm in all the experiments.

The whole set of stable characteristic features of this structural element, namely, the small discontinuity thickness and the relatively large horizontal length, the presence of a density jump, the existence of a fluid layer without fine-structure perturbations between the density wake and the interlayer, the absence of singularities at its leading and rear edges, and its localization in the field of internal waves at the level of maximum velocity shear in the mean flow allows us to identify it as an *inner boundary flow*. These properties [the small thickness, the difference between the scales of spatial variations of the velocity field $\delta_\nu = \sqrt{\nu/N}$ and the density (or salinity) $\delta_s = \sqrt{k_s/N}$, and the large length] are typical for a large group of flows: boundary flows produced by diffusion at an impermeable obstacle [11], flows at the boundaries of the density wake [9], flows generated by the internal wave on the surface of gradient discontinuity or higher derivatives of density [14], flows on stratification discontinuities in the interaction regions of the beams of harmonic internal waves [12, 13].

The measurement of variations in the electrical conductivity by a fixed probe shows that, when a body moves, together with the generation of internal waves, a general reorganization of stratification occurs. Ahead of the body, the density gradient becomes weaker due to accumulation of the homogeneous fluid from the level of body motion in the region of blocking, and it becomes stronger behind the body because of closing of the fluid layers from remote levels. The character of the changes is illustrated by the signals of a conductivity probe fixed at the depth $h = 27$ cm (at the level 0.5 cm under the lower edge of a cylinder). The recorded signals are shown in Fig. 4. The conductivity variations $\sigma(t)$ were used to calculate the displacements of the layers $\Delta = (\sigma(z_0, t) - \sigma(z_0, t_0))/(d\sigma_0(z)/dz)$, taking into account the unperturbed gradient $d\sigma_0(z)/dz$.

The conditions of the experiments correspond to the smooth wave field: $T_b = 5.2$ sec, $D = 1.5$ cm, $U = 0.34$ cm/sec, Fr $= 0.18$, Re $= 50$, and $C = 450$ (Fig. 4a) and the pattern with suspended discontinuities: $T_b = 5.2$ sec, $D = 1.5$ cm, $U = 0.43$ cm/sec, Fr $= 0.24$, Re $= 65$, and $C = 450$ (Fig. 4b). Figure 4b also shows the theoretical calculations of particle displacements [3] (dotted curve).

Although all the curves qualitatively describe the same process, there are important differences between them. All the curves show the upstream perturbation, the abrupt change of the sign of displacements upon passage of the body, and the wave oscillations behind it, because the lighter fluid ahead of the body is replaced by the heavier fluid from the lower layers during passage. In the theory, the signal oscillates at zero level; in the experiments, it oscillates at a displaced level, whose position is determined by nonlocal effects. The

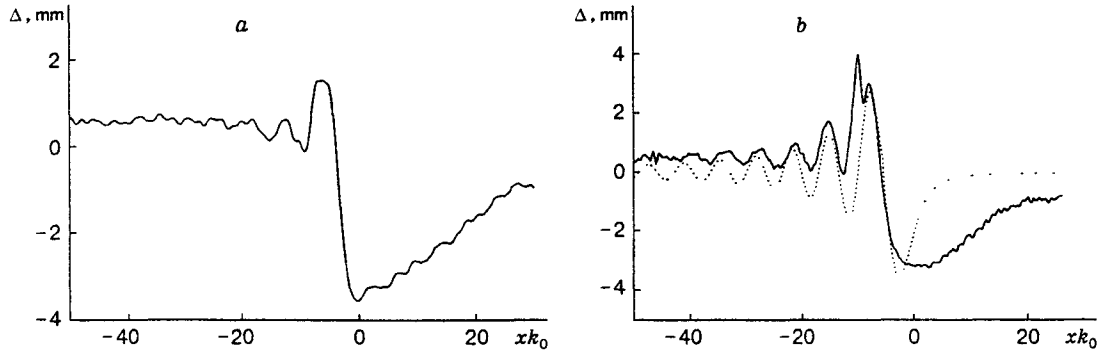

Fig. 4

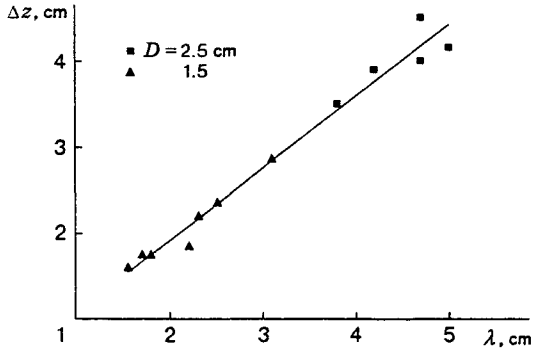

Fig. 5

character of wave oscillations (Fig. 4a) is quite uniform. The peak near the first maximum (Fig. 4b) is caused by the passage of the suspended discontinuity over the sensor.

In the experiments, the dimension of the blocking region is much greater than in the model proposed in [3] and this is reflected in the different character of the curves for $xk_0 > 0$ ($k_0 = N/U = 2\pi/\lambda$) (see Fig. 4b). In the theory and the experiment, the maximum displacements of particles in the leading perturbation nearly coincide up to the accuracy of the experiment. The character of the curves in the region of transition from unsteady to attached waves after passage of the cylinder axis is also the same.

When the probe comes across the suspended discontinuity (Fig. 4b), the sign of the derivative of displacements changes because the heavier fluid from the lower layers appears at the level of the probe. The basic character of the wave variation of the signal is restored only after a quarter of the wave period. The phase shift between the curves (Fig. 4b) is not greater than $\pi/3$ rad at the next extremum, and the calculated and observed displacements are in phase at the second and subsequent maxima.

The absolute values of the displacements are also different in the theory and the experiments. In the first and second waves, greater displacements (by 40%) are observed in the experiments, and the theoretical and experimental displacements coincide at the crests and differ at the troughs in subsequent waves; this difference grows as the wave number increases. This difference is due to neglect of the nonlocal and viscous effects in the linear theory [3]. The time of restoration of the initial stratification is quite long and is $t = 450$ sec $= 85T_b$ for the conditions of the present experiment; this time is considerably longer that the time of existence of both the identified fine structure and the attached internal waves.

The explicit connection between the geometry of the suspended discontinuity and the waves is illustrated in Fig. 5, where the distance from the plane of motion of the center of a body versus the length of the attached internal wave is shown. The results of the experiments carried out with cylinders of various diameters for three values of the buoyancy period ($T_b = 5.1$, 6.0, and 12.5 sec) lie on a single straight line

(solid line): $\Delta z = 0.27 + 0.83\lambda$ [cm]. Thus, the location of the interlayer is determined by the geometry of the field of attached internal waves, its thickness by the dissipative parameters of the medium, and its length by the energetics of the process.

The absence of a notable change in the interlayer thickness along its length may be explained by several reasons. Possibly, its real thickness in the field of density gradient is given by a small-scale parameter $\delta_s = \sqrt{k_s/N}$; then the registered size is determined by the resolution of a shadowgraph. At the same time, according to the model [14], internal waves can increase the density differences in the inner boundary flows, compensate their diffuse spreading, and maintain their uniform thickness. In this case, the real interlayer thickness is registered. Further studies are required for solving this problem.

Conclusions. Shadow visualization and contact measurements have shown the existence of isolated high-gradient interlayers in the field of attached internal waves generated by the stationary motion of a horizontal cylinder in a continuously stratified fluid. The range of the dimensionless parameters $C = 450$–1500, $\mathrm{Fr} = 0.01$–0.50, and $\mathrm{Re} = 50$–100 where they exist corresponds to the "isolated vortex patches on the wake axis" and "wake with closed high-gradient core" regimes [7, 8]. These interlayers have no specific structural features at their leading and rear edges. Their location is determined by the length of the attached internal wave. There is a fluid layer without the fine structure between the interlayers and the body. The thickness of the interlayers remains almost unchanged along their length.

These and several additional features have allowed us to consider these disturbances as the inner boundary flows inside a fluid. These structures are observed not only in the attached internal waves but also in the regions of intersection of the high-energy beams of harmonic waves [12, 13]. Thus, high-gradient interlayers may appear not only as a result of separation of stratified flows from the boundaries of an obstacle [9], degeneration of vortices [19], or turbulence [17], but also directly inside the fluid due to the nonlinear interaction between the large-scale (and more adequately understood) components of the stratified flow, namely, internal waves, flows, and vortices.

It is natural to expect that the inner boundary flows play an important role in the formation of the widely observed, so-called "fine structure" of the ambient medium. The related extended high-gradient interlayers can be a consequence of decaying turbulence. In the atmosphere and the ocean, they can be maintained by large-scale motions such as internal or inertial waves for a long time [14].

This work was partially supported by the Ministry of Science and Technology of the Russian Federation (Program for support of unique technical facilities of the Russian Federation) and by the Russian Foundation for Fundamental Research (Grant Nos. 96-05-64004 and 99-05-64980).

REFERENCES

1. W. R. Debler and C. M. Vest, "Observation of a stratified flow by means of holographic interferometry," *Proc. Roy. Soc. London, Ser. A*, **358**, 1–16 (1977).
2. J. Lighthill, *Waves in Fluids*, Cambridge Univ. Press, Cambridge (1978).
3. A. V. Aksenov, V. A. Gorodtsov, and I. V. Sturova, "Modeling of a flow of a stratified ideal incompressible fluid around a cylinder," Preprint No. 282, Inst. of Problems of Mechanics, Acad. of Sci. of the USSR, Moscow (1986).
4. V. N. Kozhevnikov, "Orographic perturbations in a two-dimensional stationary problem," *Izv. Akad. Nauk SSSR, Fiz. Atmos. Okeana*, **4**, No. 1, 33–52 (1968).
5. T. N. Stevenson, "The phase configuration of internal waves around a body moving in a density stratified fluid," *J. Fluid Mech.*, **60**, No. 4, 759–786 (1973).
6. V. I. Bukreev and N. V. Gavrilov, "Experimental study of perturbations ahead of a wing moving in a stratified fluid," *Prikl. Mekh. Tekh. Fiz.*, No. 2, 102–105 (1990).
7. D. L. Boyer, P. A. Davies, H. J. S. Fernando, and X. Zhang, "Linearly stratified flow past a horizontal circular cylinder," *Philos. Trans. Roy. Soc. London, Ser. A*, **328**, 501–528 (1989).
8. Yu. D. Chashechkin and I. V. Voeikov, "Vortex systems past a cylinder in a continuously stratified fluid," *Izv. Ross. Akad. Nauk, Fiz. Atmos. Okeana*, **29**, No. 6, 821–830 (1993).

9. I. V. Voeikov and Yu. D. Chashechkin, "Formation of discontinuities in a wake past a cylinder in a flow of stratified fluid," *Izv. Ross. Akad. Nauk, Mekh. Zhidk. Gaza*, No. 1, 20–26 (1993).
10. I. V. Voeikov, V. E. Prokhorov, and Yu. D. Chashechkin, "Microscale instability in a continuously stratified fluid," *Izv. Ross. Akad. Nauk, Mekh. Zhidk. Gaza*, No. 3, 3–10 (1995).
11. V. G. Baidulov and Yu. D. Chashechkin, "Diffusion effects on boundary flows in a continuously stratified fluid," *Izv. Ross. Akad. Nauk, Fiz. Atmos. Okeana*, **29**, No. 5, 666–672 (1993).
12. F. D. McEwan and R. A. Plumb, "On resonant amplification of finite internal wave packets," *Dynam. Atmos. Oceans*, **2**, 83–105 (1977).
13. S. G. Teoh, G. N. Ivey, and J. Imberger, "Laboratory study of the interaction between two internal wave rays," *J. Fluid Mech.*, **336**, 91–122 (1997).
14. Yu. D. Chashechkin and Yu. V. Kistovich, "Monochromatic internal waves in an arbitrarily stratified viscous fluid," *Dokl. Ross. Akad. Nauk*, **359**, No. 1, 112–115 (1998).
15. Yu. D. Chashechkin and V. A. Popov, "Color shadow method," *Dokl. Akad. Nauk SSSR*, **269**, No. 5, 1130–1133 (1981).
16. D. W. Kaufmann, *Sodium Chloride,* Reinhold, New York (1960).
17. V. S. Belyaev, "Experimental study of wave and convective flows in a stratified fluid," Candidate's Dissertation in Phys.-Math. Sci., Moscow (1984).
18. G. Schlichting, *Boundary Layer Theory*, McGraw-Hill, New York (1968).
19. V. S. Belyaev, A. M. Savinkov, and Yu. D. Chashechkin, "Dynamics of laminar vortex rings in a stratified fluid," *Prikl. Mekh. Tekh. Fiz.*, No. 1, 37–47 (1987).
20. E. Ya. Sysoeva and Yu. D. Chashechkin, "Vortex structure of a wake past a sphere in a stratified fluid," *Prikl. Mekh. Tekh. Fiz.*, No. 2, 40–46 (1986).
21. S. A. Makarov and Yu. D. Chashechkin, "Attached internal waves in fluids with exponential density distribution," *Prikl. Mekh. Tekh. Fiz.*, No. 6, 47–54 (1981).